Quantum Monte Carlo and the Holstein Model

Thomas Blommel*
North Dakota State University
(Dated: January 26, 2018)

With the advent of increasingly fast computers and their ubiquity in society, computational methods have become very important in every aspect of science. Many of these methods involve looking at a simplified model of reality, taking into account approximate forms of the major interactions in order to get more insight into the dynamics and behavior of a system. The Holstein model is such a numerical method, used used by condensed matter theorists to investigate the interactions between phonons and electrons within a solid. These interactions are the basis of the formation of charge density waves and the BCS theory of superconductivity. This paper will lay out my experiences during a summer spent in the 2017 REU program at UC Davis, under the supervision of Dr. Richard Scalettar. I will begin by laying out the basics of Monte Carlo methods and build up to the Holstein model and my findings.

I. MONTE CARLO BASICS

Monte Carlo methods were first developed by Stanislaw Ulam while working at Los Alamos National Laboratory. Soon after, John von Neumann realized the power that these methods brought and developed computers to carry out Monte Carlo calculations[1]. The core concept of Monte Carlo is that if a large number of outcomes are sampled and measured, by taking an average over these samples, accurate expectation values should be able to be measured. These outcomes are created through random processes and this dependence on randomness is how the method gets its name, after a famous casino in Monaco. In practice, one must define a system and the rules that govern the creation of new samples.

First, we look at the definition of an ensemble average for some value, A, from statistical mechanics:

$$\bar{A} = \frac{\sum_i A_i e^{-\beta E_i}}{\sum_i e^{-\beta E_i}} \tag{1}$$

where the value i represents the unique states of the system. This can be evaluated analytically if we know the entire partition function of our system, but most of the time, the system is so large, with many degrees of freedom, that it is infeasible to evaluate it. Monte Carlo methods get around this limitation by sampling a large number of states, such that the samples become representative of the large phase space. One thing to note is that in Eq. (1), each A_i is weighted by the Boltzmann weight for each individual state. This is due to the fact that higher energy states will show up less, according to the Boltzmann weight of that state. In order to take this into account, the states generated by the Monte Carlo process must be distributed according to the Boltzmann distribution. Creutz and Freedman refer to this as "importance sampling,"[2] where important states show up more often in our simulation than the unimportant ones.

Over the course of a simulation, each new state we analyze is randomly created from previous ones. At each discrete time step, many small changes to the state are suggested and the energy change, ΔE, that each small change will incur is calculated from some predefined Hamiltonian. The suggested change is then either accepted or rejected with acceptance probability

$$P(\text{accept change}) = \begin{cases} 1 & \text{if } \Delta E \leq 0 \\ e^{-\beta \Delta E} & \text{otherwise} \end{cases}. \tag{2}$$

Here, β is the inverse temperature that is defined at the beginning of the simulation, meaning each simulation is isothermal, coupled to a heat bath. This acceptance/rejection probability makes sure that important states are analyzed with the correct weighting.

A. Ising Model

One of the simplest Monte Carlo models is the Ising Model. The Ising Model is a model of ferromagnetism in solids and consists of a square lattice with a stationary particle at each lattice site that can have up or down spin. The Hamiltonian that describes our system is:

$$\hat{H} = \sum_{<i,j>} -J\sigma_i\sigma_j \tag{3}$$

where $< i, j >$ denotes all nearest-neighbor pairs, J is the coupling constant, and σ is a variable that is ± 1 based on whether the spin at a lattice site is either up or down.

At each timestep, we iterate through the lattice and try to flip each spin individually. Our results will be independent of the order in which we iterate through the lattice. When we attempt to flip a spin, we calculate the change in energy that this flip will incur. There are periodic boundary conditions, meaning a spin on an edge of the lattice is counted as a nearest neighbor to the spin on the edge of the opposite side. Using Eq. (2), the spin is either flipped or stays the same. After iterating through

* thomas.blommel@ndsu.edu

the entire lattice, the measurement process takes place. There are several important values that one would want to look at in this system, four of which are magnetism, specific heat, magnetic susceptibility and the Binder Ratio. The magnetization is given by:

$$M = \left| \sum_i \sigma_i \right|. \tag{4}$$

For the following definitions, we set $k_B = 1$ and $\beta = 1/T$. The magnetic susceptibility is how much the system will react to an outside field, and is given by

$$\chi = N\beta(\langle M^2 \rangle - \langle M \rangle^2). \tag{5}$$

The specific heat is the temperature derivative of the energy and is given statistically by:

$$C = N\beta^2(\langle E^2 \rangle - \langle E \rangle^2) \tag{6}$$

B. Ising Results

Figures 1 and 2 show the results of our Monte Carlo Ising code. We ran the simulation on a 4x4 lattice, which is small enough to allow us to do an exact enumeration scheme on the system. This enumeration scheme went through each and every possible lattice configuration and measured each of the values we are interested in and averaged them with appropriate Boltzmann weights. This enumeration thus gives us the exact values that our Monte Carlo results should converge to.

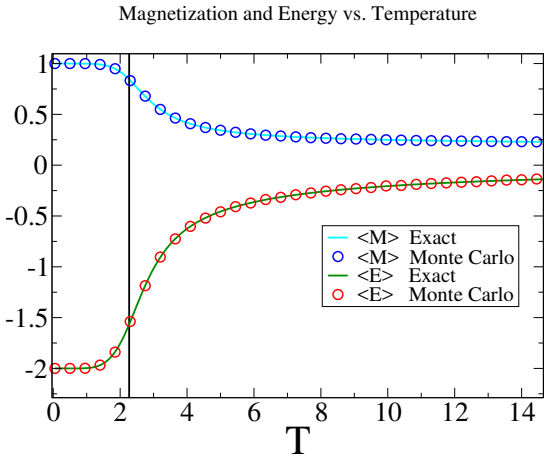

FIG. 1. The results for $\langle M \rangle$ and $\langle E \rangle$ for a 4x4 lattice of spins using the Ising Model. Both quantities are normalized to the lattice size. The Monte Carlo simulation was run for 1000 steps to allow for equilibration and then averaged over 100,000 sweeps in which every lattice site was updated at each sweep. $J = 1$.

The black vertical line is the analytic solution for the critical temperature of the 2D Square-lattice Ising Model, 2.269, found by Lars Onsager in 1944[3]. This marks the temperature at which the model goes from a magnetized to an unmagnetized state. It is important to note that the magnetization does not approach zero as the temperature increases, as would be expected. This is an artifact of the fact that we are simulating a 4x4 lattice, which is very small and was done in order to allow for the enumeration process to be feasible. The high-temperature limit will approach zero as we increase our lattice size and approach the thermodynamic limit.

Our simulations for the 4x4 Ising lattice took 100,000 sweeps to complete, which is more than the number of individual states in the model itself. In this case, for the 4x4 lattice, the exact enumeration scheme is more efficient. For the 5x5 lattice, however, a 100,000 sweep Monte Carlo simulation will be 335 times as efficient as the exact enumeration scheme.

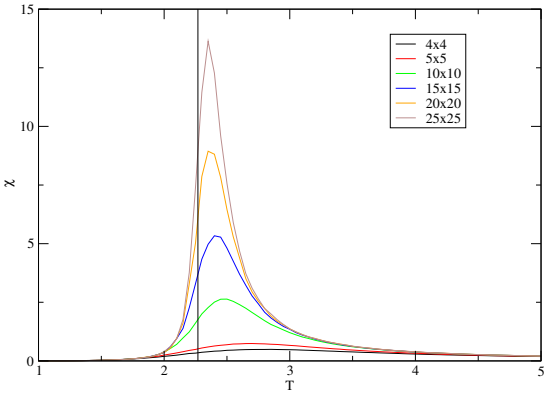

FIG. 2. Monte Carlo results for χ(magnetic susceptibility) vs. T for several lattice sizes. In thermodynamic limit, the plot should be a spike at 2.269. Note how for larger lattices, the correct value is approached and the spikes get narrower.

II. QUANTUM HARMONIC OSCILLATOR

Monte Carlo methods have been implemented with amazing success to many classical systems, such as the Ising model described above. A natural next step would be to try and implement Monte Carlo algorithms to quantum systems. For a reader who is interested, Dr. Scalettar has amazing introductory notes on several Quantum Monte Carlo systems[4]. The main difference between classical and quantum models arise in the Hamiltonian. In classical Hamiltonians the variables are all numbers, for example, ± 1 for the spins in the Ising Model. Things become more interesting when looking at quantum Hamiltonians, where we encounter operators which do not commute with each other. Taking a look at the quantum harmonic oscillator Hamiltonian, we see the famous pair of non-commuting operators, $\hat{P}$ and $\hat{X}$.

$$\hat{H} = \frac{\hat{P}^2}{2m} + \frac{m\omega^2}{2}\hat{X} \tag{7}$$

Of course, there already exist analytic solutions to the quantum harmonic oscillator, meaning we will be able

to check our code's answers and determine its accuracy. This code will also be implemented into our Holstein Model code as the phonons will be modeled as QHOs. The derivation of this method is influenced greatly by Feynman Path Integral formulation of Quantum Mechanics. In this formalism, Feynman looks at all of the possible paths a particle can take through "imaginary time" weighted by their importance[5]. In typical Monte Carlo fashion, we hope to evaluate these integrals through random sampling. This derivation was first provided by Creutz and Freedman in their 1979 seminal paper, *A Statistical Approach to Quantum Mechanics*[2]. The derivation I present is from Dr. Scalettar's notes[4]. To start out, we must determine a form of the partition function for our Hamiltonian.

$$Z = Tr[e^{-\beta \hat{H}}] \tag{8}$$

Note that $e^{-\beta \hat{H}}$ bears a striking resemblance to the quantum time evolution operator, $e^{-\frac{it}{\hbar}\hat{H}}$. Thus, motivated by Feynman, we can treat β as our imaginary time in this statistical treatment. Unfortunately, we cannot break apart this exponential, as $\hat{P}$ and $\hat{X}$ do not commute, and so we must proceed by making an approximation: we discretize β (our imaginary time) into L pieces, each of length $\Delta\tau$, giving $\beta = L\Delta\tau$. This is what is known as a Trotter approximation, and gives us

$$Z_{tr} = Tr[e^{-\Delta\tau \hat{P}^2/2m} e^{-\Delta\tau m\omega^2 \hat{X}^2}]^L. \tag{9}$$

In the limit of $\Delta\tau \to 0$, we recover Feynman's formalism and the exact solution.

Since we are looking to simulate a physical QHO system, we will be working with positional eigenstates. It then makes sense that we evaluate our trace over the positional states, giving

$$Z_{tr} = \int dx_1 \langle x_1 | [e^{-\Delta\tau \hat{P}^2/2m} e^{-\Delta\tau m\omega^2 \hat{X}^2}]^L | x_1 \rangle. \tag{10}$$

Using the relation,

$$\int dx \ |x\rangle\langle x| = 1 \tag{11}$$

We can insert a complete set of positional states in between each of the L exponential factors, giving

$$\begin{aligned} Z_{tr} = &\int dx_1 dx_2 ... dx_L \langle x_1 | e^{-\Delta\tau \hat{P}^2/2m} e^{-\Delta\tau m\omega^2 \hat{X}^2} | x_2 \rangle \\ &\langle x_2 | e^{-\Delta\tau \hat{P}^2/2m} e^{-\Delta\tau m\omega^2 \hat{X}^2} | x_3 \rangle ... \\ &\langle x_L | e^{-\Delta\tau \hat{P}^2/2m} e^{-\Delta\tau m\omega^2 \hat{X}^2} | x_1 \rangle \\ = &\int dx_1 dx_2 ... dx_L \exp[-\frac{1}{2} m\omega^2 \Delta\tau \sum_{l=1}^{L} x_l^2] \\ &\langle x_1 | e^{-\Delta\tau \hat{P}^2/2m} | x_2 \rangle ... \langle x_L | e^{-\Delta\tau \hat{P}^2/2m} | x_1 \rangle. \end{aligned} \tag{12}$$

In the second equality sign, we simply evaluated the $\hat{X}$ operator on the position eigenstates and got out the number values, x_l. We have yet another problem, as we now have $\hat{P}$ operators acting on position states. To remedy this, we use Eq. (11), this time inserting complete sets of momentum states. Each one of the remaining matrix elements can be evaluated as such:

$$\begin{aligned} \langle x_l | e^{-\Delta\tau \hat{P}^2/2m} | x_{l+1} \rangle &= \int dp \langle x_l | e^{-\Delta\tau \hat{P}^2/2m} | p \rangle \langle p | x_{l+1} \rangle \\ &= \int dp \ e^{-\Delta\tau p^2/2m} e^{ip(x_l - x_{l+1})} \\ &= \sqrt{\frac{2m\pi}{\Delta\tau}} e^{-\frac{1}{2} m\Delta\tau [(x_l - x_{l+1})/\Delta\tau]^2} \end{aligned} \tag{13}$$

We have now removed our momentum dependence from our partition function. The velocity part of our kinetic energy operator comes out to be the difference in position between adjacent time slices, divided by $\Delta\tau$. We drop the prefactor, as we can see that it will cancel out when we measure expectation values.

Our final result is our partition function is now approximated to arbitrary precision by the classical position,

$$\begin{aligned} Z_{tr} &= \int dx_1 dx_2 ... dx_L \ e^{-\Delta\tau S_{cl}} \\ S_{cl} &= \frac{1}{2} m\omega^2 \sum_l x_l^2 + \frac{1}{2} m \sum_l \left(\frac{x_l - x_{l+1}}{\Delta\tau} \right)^2 \end{aligned} \tag{14}$$

S_{cl} is called the classical action, and is what we use in our simulation to calculate the acceptance probability for a certain suggested move. The ΔE in Eq. (2) is replaced by ΔS_{cl}. This result can be generalized easily to the anharmonic oscillator, which has no analytic solution, using the same derivation presented above.

Analyzing our action, we notice that what was once a one dimensional problem, a quantum harmonic oscillator, has now turned into a two dimensional problem in which we have a line of classical harmonic oscillators that are coupled together through some quadratic potential we can think of as a spring potential. A diagram of what this can be visualized as is shown in Fig. 3. This is a general truth for all quantum systems: A quantum Hamiltonian of dimension D will map to a classical action of D+1 dimensions, where the extra dimension is imaginary time.

A. QHO results

I spent a portion of time writing a QHO Monte Carlo code and then comparing the results with the known analytic solutions. I looked at particularly the expectation values of the potential and kinetic energy vs. temperature, which, according to the Virial Theorem, should be equal. Fig. 4 shows the results of my code alongside the analytic solution. As is evident from the graph, smaller values of $\Delta\tau$ give better agreement with the actual values, but smaller $\Delta\tau$ values also incur larger computa-

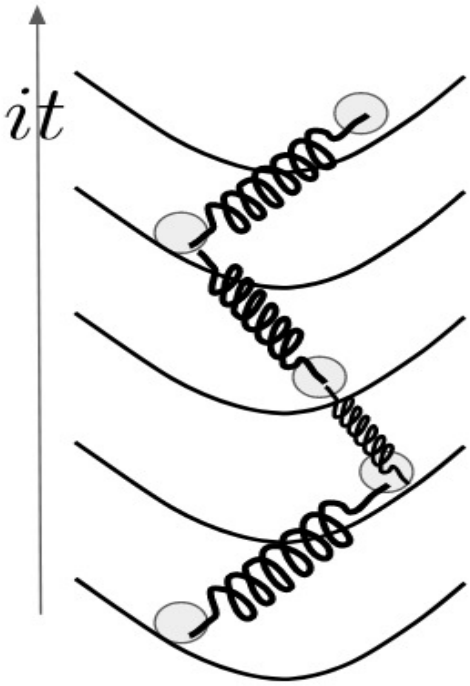

FIG. 3. A snapshot visualization of what our system may look like within the simulation

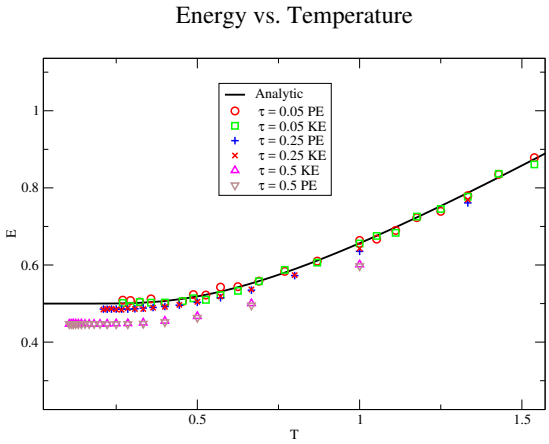

FIG. 4. Analytic and simulation results for the expectation of kinetic and potential energy for the quantum harmonic oscillator.

tional expenses, as more imaginary time slices must be considered.

III. HOLSTEIN MODEL

The Holstein model is a simplified model that aims to describe the interactions between phonons and fermions (electrons) within a solid. I will use the term electron but the reader should be aware that the model does not take into account charge interactions between particles. The Holstein model treats each lattice point as a nucleus that can wiggle in position, such as they do in real solids. These phonons are modeled as QHOs. Electrons are present in the simulation and can hop between lattice sites, yet there are only allowed to be two at each site, in accordance with the Pauli Exclusion Principle. The complete Hamiltonian is given by:

$$\begin{aligned}\hat{H} = &- t\sum_{i,j,\sigma}(c^{\dagger}_{i\sigma}c_{j\sigma} + c^{\dagger}_{j\sigma}c_{i\sigma}) - \mu\sum_{i} n_i \\ &+ \lambda\sum_{i} n_i\hat{x}_i + \sum_{i}\left(\frac{1}{2}\hat{p}_i^2 + \frac{\omega^2}{2}\hat{x}_i^2\right)\end{aligned} \tag{15}$$

This Hamiltonian will take a bit of explaining in order to fully understand. First, $c^{\dagger}_{i\sigma}$ and $c_{i\sigma}$ are operators which destroy and create an electron with spin σ at lattice site i, respectively. The first term in the Hamiltonian acts as the kinetic energy operator, it moves an electron from site i to j, which increases the energy by t, a value that is almost always set to 1. The next term is a chemical potential μ and the n_i is the number of electrons at site i. This term allows us to tune the amount of electrons we have in our system. Because we are interested in special phases called charge-density waves, we always run our simulations such that there are, on average, one electron per lattice site. The third term describes the coupling between phonons and electrons; λ is a constant which sets the strength of this coupling. Analyzing this term closer shows that it is energetically advantageous for phonons to stretch (in the negative direction) when there is an electron (or two) on the lattice site. Finally, the last term is the QHO Hamiltonian we described above, which governs the phonons at each lattice site.

It was my job to investigate the dependence of the critical temperature on parameters such as the electron-phonon coupling constant and the phonon frequency. Dr. Scalettar mentioned several times that there is a large false assumption within the Holstein literature that states that the dynamics and properties of a system depend simply on the ratio λ^2/ω. What we set out to show is that this is not true by finding the critical temperatures at different values for λ^2/ω for several different values for λ and showing they do not match up. Our results would show how well this value actually does at characterizing the system.

Just as any good researcher should do before using a code supplied to them, I first checked its results to analytic solutions I found. The Holstein Model itself has no analytic solution, but in two limiting cases one can solve it exactly. The first limiting case is when the kinetic energy term, t, is set to zero. This is known as the Single-Site Holstein model as there is no movement of electrons from site-to-site. In this limiting case, we can find solutions for the expectation value of electron density. I also adapted my QHO code from earlier into my

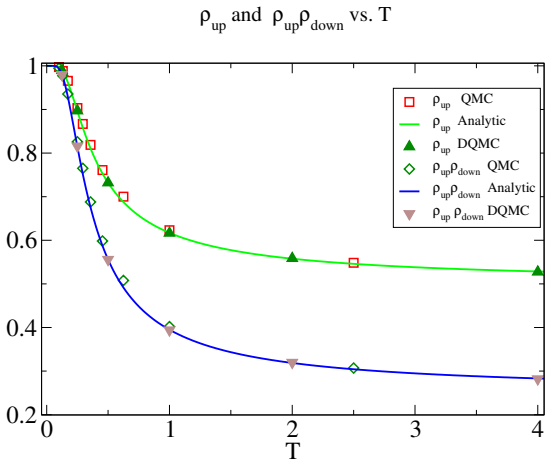

FIG. 5. Three results for the expectation value of electron density in the Single-Site Holstein model. Solid lines are analytic solutions, solid data points are from the code I was given and the hollow data points are from my own code. All show very good agreement with each other. $\mu = 0.2$

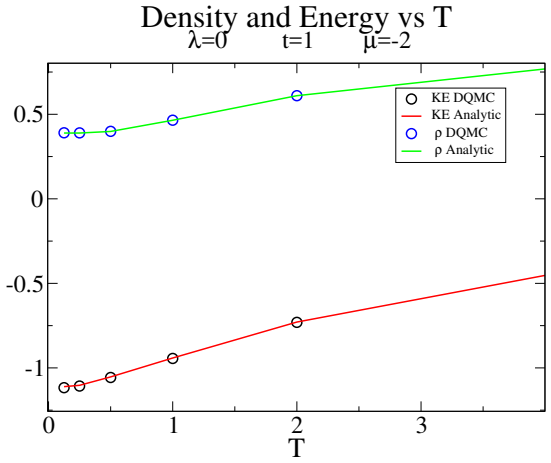

FIG. 6. Analytic and simulation results for the non-interacting phonons and electrons. Good agreement is shown, giving confidence to the accuracy of the DQMC code.

own Single-Site Holstein code. The results for this first test of the code are shown in Fig. 5.

The second limit in which I tested the code is where $\lambda = 0$, that is, where there is no interaction between phonons and electrons. I did not write my own code for this limit, but I did compare the results of the code I was given to the analytic solution. These results are shown in Fig. 6 and show great agreement for both density and energy.

A. Connection to BCS Theory

The BCS theory of superconductivity is a very successful microscopic theory of the origins of superconductivity.[6] It was first presented in 1957 by Bardeen, Cooper, and Schrieffer, who were all later awarded the Nobel Prize for the work in 1972. The basis of the theory is that at low temperatures, the interactions between electrons and phonons on the lattice become significant and lead to the formation of Cooper pairs. These Cooper pairs act as bosons and form a Bose-Einstein condensate within the material, which leads to the superconductive properties we encounter. The mechanism for the formation of Cooper pairs in BCS theory and in the Holstein model are the same. An electron will attract a nucleus (lattice site) towards itself within the material. This attraction is accounted for in the third term of our Hamiltonian. This attraction moves the nucleus farther from its equilibrium position at the lattice site. Another electron will then be attracted to this positive charge as it moves closer and will hop onto the lattice site. Thus, we have two electrons on such a lattice site, which is our Cooper pair. This causes further stretching of the phonon and it becomes more and more energetically unfavorable for either of the electrons to leave the lattice site and they become, in a sense, bound.

B. Charge Density Waves

Superconducting phases do occur in the Holstein model, but they occur when there are less electrons on the lattice which are free to move around without complications arising from the Pauli Exclusion Principle. What we are interested in though, is a phase called a charge-density wave. This occurs when the system is at half-filling, meaning there is, on average, one electron per lattice site. The charge density wave phase is characterized by an alternating pattern of sites with no electrons and two electrons. A diagram of what this looks like in a 2D system is shown in Fig. 7.

These phases are interesting because they occur in real materials and often compete with superconducting phases. Knowledge about how these phases form may help us in the design of new materials in which the superconducting phase occurs at larger amounts of conditions. A real material where this competition is of particular interest is $Ba_{1-x}K_xPbBiO_3$. The relative concentrations of Ba and K change the phase diagram and the conditions at which superconductivity or CDW phases occur.

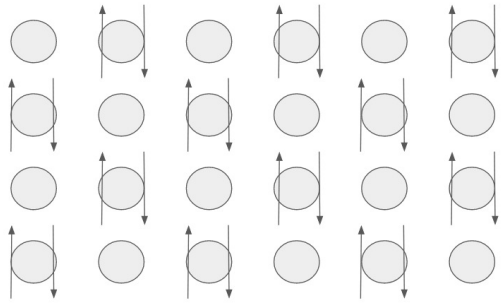

FIG. 7. Diagram of a charge density wave state in the Holstein model. Circles are the lattice sites and the up and down arrows represent electrons with spins up and down.

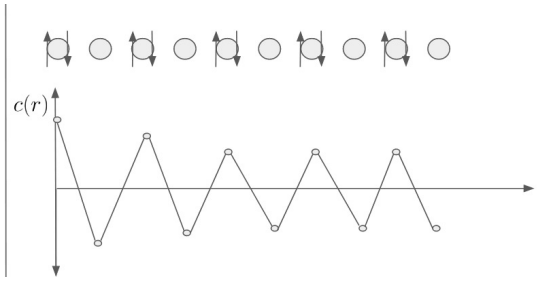

FIG. 8. Correlation function for a CDW state. At long ranges, the sites an even number away from our origin are positively correlated, while the odd sites are negatively correlated.

C. CDW Structure Factor

In order to determine whether or not the system is in a CDW state, we measure what is called the CDW structure factor. We first define a correlation function for some operator $\hat{O}$ as

$$c(r) = \langle \hat{O}_{r_0} \hat{O}_{r_0+r} \rangle \tag{16}$$

Where r_0 is some origin lattice site and $\langle\rangle$ denotes an ensemble average. This correlation function behaves as:

$$c(r) = \begin{cases} e^{-\frac{r}{\xi}} & \text{if } T > T_c \\ r^{-p} & \text{if } T = T_c \\ const. & \text{if } T < T_c \end{cases}. \tag{17}$$

Fig. 8 shows an example of a lattice which is in a CDW state, meaning that $T < T_c$ and the correlation function should become constant at long ranges. In order to calculate the structure factor, we take the Fourier Transform of the correlation function and analyze the $q = \pi$ mode

$$SF(q) = \sum_r c(r) e^{iqr}. \tag{18}$$

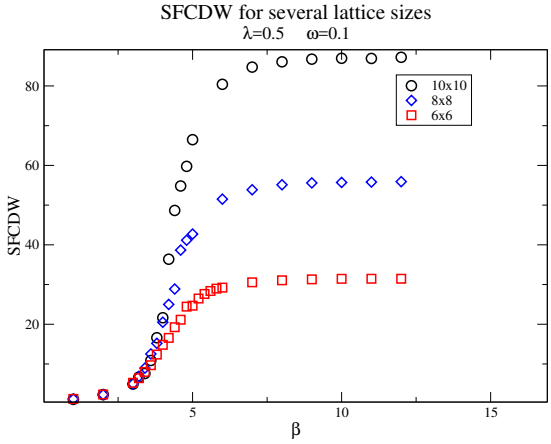

FIG. 9. Structure Factor vs inverse temperature for three different lattice sizes. Each data point comes from an individual simulation.

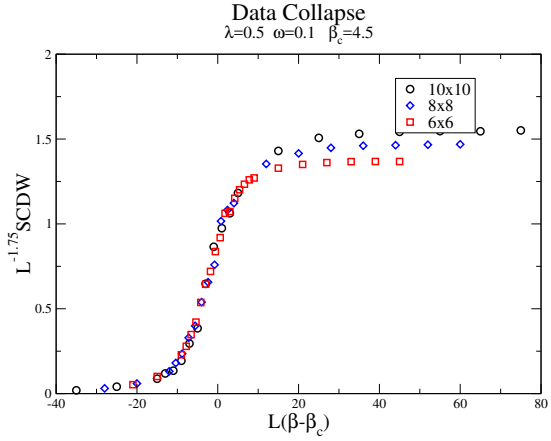

FIG. 10. Data collapse. All data points around the critical temperature lie nicely on top of each other. The low temperature (high β) regime is not expected to collapse.

D. Results

We ran our simulations for three different lattice sizes: 6x6, 8x8 and 10x10. Each lattice size was ran for 20 different temperatures. An example of a plot of our data is given in Fig. 9.

The critical temperature is the temperature at which the phase transition into the CDW occurs. In order to determine this temperature, we do a data collapse on the data presented in Fig. 9. This type of data collapse is commonplace in condensed matter theory for finding the critical temperatures of certain systems. This data collapse is done such that the results from each of the lattice sizes end up lying on top of each other. This is done buy an algorithm that determines the β_c that minimizes the distance between data points. The collapse for the data presented in Fig. 9 is given in Fig. 10. Note the scaling factors that are used and shown on the axis labels.

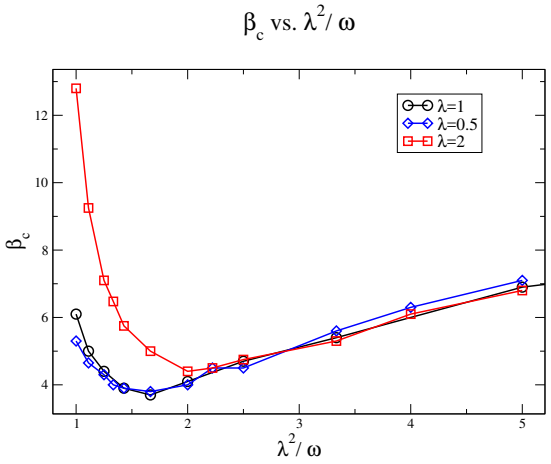

FIG. 11. The final goal of my project: to show the dependence of the critical temperature on the value λ^2/ω

Once we got all the β_c for all our values, we put them all on a β_c vs. λ^2/ω plot. If one were to believe that λ^2/ω was a good determinant of the properties of the system, one would expect that the curves for different values of λ would lie on top of each other. What we found was that this was actually quite a good assumption to make in the regime of low ω values, as shown in Fig. 11. There were large deviations though, in the high ω regime.

E. Conclusions

We originally set out to test the assumption that the value λ^2/ω determines the dynamics and properties of a system in the Holstein model. This assumption is prevalent in the community and literature, so to either provide evidence for or to dispel this assumption is rather important. We tested this by finding the critical temperature at 12 different values of λ^2/ω with 3 different λ values for each. We found that in the limit that $\lambda^2/\omega > 2$, the β_c for all three simulations were very close. However, outside this region, there were large divergences for the different λ values. This finding shows that the assumption that λ^2/ω is a good predictor of the properties of a system may be valid for some values, but fails in the high-ω limit.

[1] N. Metropolis, "The Beginning of the Monte Carlo Method," *Los Alamos Science Special Issue*, 1987.

[2] M. Creutz and B. Freedman, "A Statistical Approach to Quantum Mechanics," *Annals of Physics*, vol. 132, no. 2, pp. 427 – 462, 1981.

[3] L. Onsager, "Crystal statistics. i. a two-dimensional model with an order-disorder transition," *Phys. Rev.*, vol. 65, pp. 117–149, Feb 1944.

[4] R. T. Scalettar, "World-Line Quantum Monte Carlo." www.phys.uri.edu/nigh/QMC-NATO/webpage/abstracts/scalettar.ps.

[5] R. Feynman, "Principles of least action in quantum mechanics." https://cds.cern.ch/record/101498/files/Thesis-1942-Feynman.pdf.

[6] J. Bardeen, L. N. Cooper, and J. R. Schrieffer, "Theory of superconductivity," *Phys. Rev.*, vol. 108, pp. 1175–1204, Dec 1957.